Eur. Phys. J. B **58**, 1–10 (2007)
DOI: 10.1140/epjb/e2007-00197-0

THE EUROPEAN PHYSICAL JOURNAL B

Low temperature properties of the Kondo insulator FeSi

M.S. Figueira[1,a] and R. Franco[2]

[1] Instituto de Física, Universidade Federal Fluminense, Av. Litorânea s/n, 24210 − 346 Niterói-RJ, Brazil
[2] Departamento de Física, Universidad Nacional de Colombia, Ciudadela Universidad Nacional, Bogotá, Colombia

Received 9 February 2007 / Received in final form 31 May 2007
Published online 13 July 2007 –

Abstract. In this paper we study the low temperature (T) properties of the Kondo insulator FeSi within the X-boson approach. We show that the ground state of the FeSi is metallic and highly correlated with a large effective mass; the low temperature contributions to the specific heat and the resistivity are of the Fermi-liquid type. The low temperature properties are governed by a reentrant transition into a metallic state, that occurs when the chemical potential crosses the gap and enters the conduction band, generating a metallic ground state. The movement of the chemical potential is due to the strong correlations present in the system. We consider the low temperature regime of the Kondo insulator FeSi, where the hybridization gap is completely open. In this situation we identify the two characteristic temperatures: the coherence temperature T_0 and the Kondo temperature T_{KL}. In the range $T < T_0$, we identify a regime characterized by the formation of coherent states and Fermi-liquid behavior of the low temperature properties; in the range $T_{KL} > T > T_0$, we identify a regime characterized by an activation energy. Within the X-boson approach we study those low temperature regimes although we do not try to adjust parameters to recover the experimental energy scales.

PACS. 75.30.Mb Valence fluctuation, Kondo lattice, heavy-fermion phenomena – 71.10.Ay Fermi-liquid theory and other phenomenological models – 73.61.Ng Insulators

1 Introduction

The Kondo insulators (KI) have been studied intensively since their classification as highly correlated insulators systems by Aeppli and Fisk [1]. Among the large number of metallic rare earths and actinide compounds there are some of then that present insulator behavior ($Ce_3Bi_4Pt_3$, SmB_6, UNiSn, FeSi, etc.). These materials exhibit a very small gap and it is believed that the gap arises in the lattice, from the hybridization between the localized electrons (f-electrons) and the conduction electrons (c-electrons) [2]. The KI's usually have cubic symmetry and a mixed-valence character for the f-elements [2,3]. The main theoretical interest in these materials is due to the existence of large many-body renormalizations. The gaps inferred from optical, magnetic, transport and thermodynamics properties are almost an order of magnitude smaller than those obtained by band computation techniques [2,4]. Also the spectral densities inferred from high resolution angle-resolved photoemission [5] (ARPES) indicate the existence of an extremely temperature dependent narrow f feature in the electronic density of states close to the top of the valence band, which can be identified with a band of heavy quasi-particles. The strong Coulomb correlations associated with the f character of the states at both edges of the band gap, are also assumed to be responsible for the universal temperature dependencies exhibited by this class of materials [4].

Due to their unusual thermodynamic properties the compound FeSi [6] is also classified as a Kondo insulator. The FeSi specific heat C_v, presents a broad maximum at around 250 K. The magnetic susceptibility χ rises rapidly in the region where C_v is maximum and also presents a maximum at approximately 500 K, but at low temperatures, presents a minimum at around 90 K and grows more than two orders of magnitude as the temperature is lowered below 1 K [7–12].

It was showed by Varma [13] that Kondo rare earth compounds with insulating ground state must, except for a small probability, be mixed valence (he also includes FeSi in his discussion). In the case of FeSi, the ground state is Fe^{2+} ($d6$) hybridized with Si. The local symmetry is threefold so that the angular momentum is quenched, the ground state spin is zero. The lowest-energy excitation is a multiparticle-hole excitation to an Fe^{1+} ($d7$) state ($S = 3/2$), which is hybridized to Si bands. The mixed valence occurs because the configurations (Fe^{2+}–Fe^{1+}) boundary lie, very close to the chemical potential, in the gap of the compound. In particular he showed that in this class of mixed valence materials, included FeSi, both the RKKY and the double exchange interactions vanish.

Recently the interest on this compound was renewed by the discovery that FeSi doped with Co or Mn shares

[a] e-mail: figueira@if.uff.br

the very highly anomalous Hall conductance of the magnetic semiconductor (GaMn)As [14], which presents the possibility of using doped Co or Mn-FeSi with transition metals as a potential application as injectors for spintronics applications due to the large magnetic-field effects on its electrical properties [15].

Paschen et al. [10] pointed out that the ground state of FeSi is not so simple, with part of the magnetic moments interacting between themselves and part remaining paramagnetic down to at least 50 mK. Recently a very complete work on the transport and magnetic properties of FeSi was performed by Glushkov and co-workers [16]. Their results indicate that below 100 K a metallic heavy fermion state is formed, as a result of fast fluctuations in the density of states and as we have shown in this work, this metallic ground state governs the low temperature properties of the system. By decreasing the temperature more, down to the Curie temperature $T_C \simeq 15$ K the system suffers a ferromagnetic transition accompanied by the formation of nanosize anisotropic ferromagnetic regions (ferrons) and finally at $T_m \simeq 7$ K the system suffers a transition to the ferron state for a spin-glass ground state. Our model is not addressed to describe these rich magnetic behaviors because we only consider the paramagnetic solutions of the model.

Another set of magnetization measurements, performed by Sluchanko et al. [17], for high quality single crystals of FeSi in a wide range of temperatures (1.5–300 K) and a magnetic field (up to 120 KOe) showed that the increase of the magnetic susceptibility observed in FeSi at temperatures below 70 K could be associated with the evolution of the Pauli-like susceptibility paramagnetic contribution from the narrow conduction band at the Fermi level. Finally Lunkenheimer et al. [9] performed a series of measurements of AC conductivity of polycrystalline FeSi at temperatures 80 mK $\leq$ T $\leq$ 450 K and frequencies 20 Hz $\leq \nu \leq$ 1 GHz and obtained a result that shows that at very low temperatures, and in the metallic side, the dominant charge carriers behave as band-like states and there is no signal of hopping conductivity. They showed that below 4.5 K the dielectric constant increases by a factor of 10 when the temperature was lowered down to 1.6 K. They concluded that this strong increase could indicates a transition into a metal-like state at low temperatures. This interpretation was also suggested by the experimental results of Hunt et al. [8] and Chernikov et al. [11].

It has been suggested by Degiorgi [18] that the low temperature regime of FeSi is governed by an impurity band inside the gap, with residual impurity concentration at the level of 10^{19} cm^{-3}, what suggests a metallic ground state for this material. In the same line, Paschen et al. [10] experimental results of the low temperature specific heat, also suggest a metallic ground state but with electrons highly correlated, with an effective-mass ratio of approximately 900 and also suggest that the origin of this metallic ground state could be an impurity band formed in the gap with a "spectacularly" narrow band width.

Schlottmann [19] considered a finite concentration of Kondo holes forming an impurity band in the Kondo insulator gap. To describe the system he employed the Anderson lattice model within the $U2$ expansion approximation [20], he neglected the $\boldsymbol{k}$ dependence of self-energy and contrary to the X-boson, this approximation is only valid for small Coulomb correlation U values. He showed that a finite concentration of Kondo holes gives rise to an impurity band in the gap which pins the Fermi level and calculated the charge susceptibility and linear T specific heat coefficient γ, that correspond to an effective-mass enhancement of 15–20 over the mass of the conduction electrons. It is important to emphasize that the experimental results of Paschen et al. [10] indicate, in the very low temperature regime, an enhancement of the effective-mass ratio of approximately 900, which agrees very well with the results obtained by the present X-boson treatment.

On the other hand Arushanov et al. [21] performed measurements of magnetization and magnetic susceptibility to determine the FeSi band parameters. They applied the Kamimura model [22] to explain the low temperature Curie-Weiss susceptibility, which is attributed, by several authors [4,10,18], to localized Anderson impurities in the gap. The Kamimura model takes into account the intrasite interactions between the Anderson localized electrons and their calculations showed that the contribution to the magnetic susceptibility from the single occupied Anderson localized states in their FeSi samples were completely negligible. According to their results the temperature dependence of χ in the temperature range of 5–300 K could be explained by the contribution from the temperature dependent parts due to paramagnetic centers and due to the carriers excited thermally in the intrinsic conductivity region.

Another possible scenario for the insulator-metal transition in doped Kondo insulators was proposed recently by Peche et al. [23]. They studied the Kondo insulator compound $(Ce_{1-x}La_x)_3Bi_4Pt_3$, where the impurity band formed inside the gap drives the position of the chemical potential μ and controls the properties of the system. When the La concentration attains a critical value, μ enters the conduction band and the system becomes metallic. On the other hand, the experimental measurements indicate that a very small concentration of impurities ($x \simeq 0.005$) is enough to produce the insulator-metal transition [24], suggesting that the insulator-metal transition does not take place within the impurity band, because according to percolation theory [25] a much larger concentration of impurities it is necessary so that the impurity band becomes a conductor.

In this work we propose a model to describe the Kondo insulator FeSi, in the low temperature regime, where the hybridization gap is completely open. The model is consistent with the scenario indicated by the experimental works of Lunkenheimer et al., Hunt et al. and Chernikov et al. [8,9,11], where a reentrant transition into a metallic state, at very low temperatures is suggested. In our case, the insulator-metal transition in FeSi is driven by strong

Coulomb correlations that occur when the chemical potential μ crosses the gap and enters in the lower conduction band, generating a metallic ground state. For simplicity we do not consider the role of the impurity band as made by Peche et al. [23]. In our model the existence of an impurity band to produce the insulator-metal transition is not necessary, although the interplay between strong correlations and disorder originated from localized states of the impurity band, inside the gap, and in the intermediate to low temperature range, play a relevant role in the properties of FeSi, once they contribute to change the position of the chemical potential μ inside the gap.

The periodic Anderson model (PAM) at half-filling has been extensively used to study the Kondo insulators [4]. This model has an indirect hybridization gap Δ_{ind} between bands of localized and conduction electrons and a direct gap Δ_{dir} associated with the minimum energy for interband transitions [26]. We have recently studied the FeSi using the atomic approach [27,28] and we were able to adjust simultaneously the static conductivity, the resistivity and the dynamical conductivity to the experimental results, and we obtained a fair agreement with the experimental results. The PAM with $U \to \infty$ has been suggested as an adequate model to study the KI [1], and in particular the compound $Ce_3Bi_4Pt_3$ was studied employing the slave-boson technique in the mean field approximation (SBMFT) [29–31]. The SBMFT is designed to work in the Kondo regime, at low temperatures, because it captures the strong spin fluctuations, characteristic of the Kondo limit, but the method presents problems to describe temperature properties because it produces a spurious second-order phase transition at the Kondo temperature T_{KL} [30, 32–34] and at temperatures $T > T_{KL}$ the conduction and localized electrons decouple, which is an unphysical result.

In this work we employ the X-boson method [34,35] to study the PAM in the limit of infinite Coulomb repulsion $U \to \infty$. Recently we employed the X-boson method to describe thermodynamics properties of metallic heavy fermions compounds and we have obtained results in qualitative agreement with experimental works and other theoretical techniques [36]. The X-boson includes the correlation in an analog way to the slave boson mean field theory (SBMFT), but do not present the well known spurious second order temperature phase transition of the SBMFT and carry some of the local quantum fluctuations that are absent in the quasi-particle Green's functions of this method; therefore, its applicability is not restricted to the extreme Kondo region, it is a good approximation to describe the intermediate valence regime, characteristic of the Kondo insulators. The method satisfies the important property of completeness, that is not satisfied, for example, by several approaches based on the equation of movement method (EOM), that describes the Kondo peak with a di-gamma family of approximations [37]. Besides this, the X-boson does not present several thermodynamic inconsistencies, characteristic of Hubbard I-like approximations and the SBMFT approach; the X-boson solution is obtained by solving a self-consistent equation system, where the localized energies are renormalized in such a way that the solution lies in a free Helmholtz energy minimum [35]. But the X-boson also presents limitations that should be taken into account; the formalism does not incorporate a finite imaginary part of the self-energy (although the method can be extended to include such effects). Therefore, the method is not adequate to describe the transport properties of the high temperature regime ($T > T_{KL}$); those effects will lead the gap to close and the compound becomes a dirty metal.

The finite lifetime effects were considered by Fu and Doniach [38] in their study of the Kondo insulators. They described the intermediate to high temperature regime of the FeSi, employing a two Hubbard band model within the $U2$ expansion approximation [20], but with the $\boldsymbol{k}$ dependence of the self-energy neglected. The results obtained were in good agreement with the experimental magnetic susceptibility and the optical conductivity, but the model did not explain the problem of the missing spectral density in the optical conductivity reported by Schlesinger et al. [7].

We restrict our study to the low temperature properties of FeSi, where the X-boson approach is a good approximation, and in particular we calculate the specific heat, resistivity and magnetic susceptibility in this temperature regime. In Section 2 we present a brief description of the X-boson method with the relevant formulas. In Section 3 we derive the formulas, within the X-boson approach, used to calculate the transport properties: specific heat, resistivity and susceptibility. In Section 4 we discuss the results and finally in Section 5 we present the conclusions.

2 Model and method: the X-boson approach

To study the PAM Hamiltonian in the $U = \infty$ limit [39, 40], the f-levels with double occupation are projected out from the space of the local states by employing the Hubbard X operators [41,42] and we obtain

$$H = \sum_{\mathbf{k},\sigma} \varepsilon_{\mathbf{k},\sigma} c^{\dagger}_{\mathbf{k},\sigma} c_{\mathbf{k},\sigma} + \sum_{\sigma,f} E_{f,\sigma} X_{f,\sigma\sigma} + \sum_{\mathbf{k},\sigma} \left(V_{f,\mathbf{k},\sigma} X^{\dagger}_{f,0\sigma} c_{\mathbf{k},\sigma} + V^{*}_{f,\mathbf{k},\sigma} c^{\dagger}_{\mathbf{k},\sigma} X_{f,0\sigma} \right). \quad (1)$$

The first term of the equation represents the Hamiltonian of the conduction electrons (c-electrons), associated with the itinerant electrons (s, p and d orbitals). The second term describes the localized f levels and the last one corresponds to the interaction between the c-electrons and the f-electrons via hybridization between the f and c states. This Hamiltonian can be treated by the X-boson approach [34,35] for the lattice case, and the cumulant Green's function (GF) are then given by

$$G^{ff}_{\mathbf{k}\sigma}(z) = \frac{-D_{\sigma}\left(z - \varepsilon_{\mathbf{k}\sigma}\right)}{\left(z - \widetilde{E}_{f,\sigma}\right)\left(z - \varepsilon_{\mathbf{k}\sigma}\right) - |V_{\sigma}(\mathbf{k})|^2 D_{\sigma}}, \quad (2)$$

$$G^{cc}_{\mathbf{k}\sigma}(z) = \frac{-\left(z - \widetilde{E}_{f,\sigma}\right)}{\left(z - \widetilde{E}_{f,\sigma}\right)\left(z - \varepsilon_{\mathbf{k}\sigma}\right) - |V_{\sigma}(\mathbf{k})|^2 D_{\sigma}}, \quad (3)$$

and

$$G^{fc}_{\mathbf{k}\sigma}(z) = \frac{-\ D_\sigma V_\sigma(\mathbf{k})}{\left(z - \widetilde{E}_{f,\sigma}\right)(z - \varepsilon_{\mathbf{k}\sigma}) - |V_\sigma(\mathbf{k})|^2 D_\sigma}, \quad (4)$$

where $z = \omega + i\eta$, with $\eta \to 0^+$. The correlations appear in the X-boson approach through the quantity $D_\sigma = R + n_{f,\sigma}$, where $R = \langle X_{0,0}\rangle$. This simple factor introduces essential differences with the SBMFT [34,35] and these GF cannot be transformed into those of two hybridized bands of uncorrelated electrons with renormalized parameters, as it is done in the SBMFT.

In the X-boson approach the quantity D_σ must be calculated self-consistently through the minimization of the corresponding thermodynamic potential with respect to the parameter R, at the same time $\widetilde{E}_{f,\sigma} = E_{f,\sigma} + \Lambda$, where Λ is a Lagrange multiplier. When the total number of electrons N_t, the temperature T and the volume V_t are kept constant one should minimize the Helmholtz free energy F, but the same minimum is obtained by employing the thermodynamic potential $\Omega = -k_B T \ln(\mathcal{Q})$, (where $\mathcal{Q}$ is the grand partition function) while keeping T, V_t, and the chemical potential μ constant (this result is easily obtained by employing standard thermodynamic techniques). In the X-boson method the grand thermodynamic potential is [34,35]

$$\Omega = \overline{\Omega}_0 + \frac{-1}{\beta}\sum_{\mathbf{k},\sigma,\pm} \ln\left[1 + \exp(-\beta\ \omega_{\mathbf{k},\sigma}(\pm))\right] + N_s\ \Lambda(R-1), \quad (5)$$

where

$$\overline{\Omega}_0 = -\frac{N_s}{\beta}\ln\left[\frac{1 + 2\exp(-\beta\widetilde{E}_f)}{(1+\exp(-\beta\widetilde{E}_f))^2}\right], \quad (6)$$

$\beta = 1/k_B T$, and k_B is the Boltzmann constant.

After the minimization of the thermodynamic potential Ω with respect to the R parameter we obtain

$$\Lambda = \frac{-1}{N_s}\sum_{\mathbf{k},\sigma}\frac{|V_\sigma(\mathbf{k})|^2\left[n_F\left(\omega_{\mathbf{k},\sigma}(+)\right) - n_F\left(\omega_{\mathbf{k},\sigma}(-)\right)\right]}{\sqrt{\left(\varepsilon_{\mathbf{k},\sigma} - \widetilde{E}_{f,\sigma}\right)^2 + 4\left|V_\sigma(\mathbf{k})\right|^2 D_\sigma}}, \quad (7)$$

where $n_F(x)$ is the Fermi-Dirac distribution

$$n_F(z) = \left[1 + \exp(\beta\ z)\right]^{-1} \quad (8)$$

and N_s is the number of sites. To simplify the calculations we shall consider a rectangular conduction band of width $W = 2D$, centered at the origin, and a real hybridization constant $V_\sigma(\mathbf{k}) = V$. We then obtain

$$\Lambda = \frac{-V^2}{D}\int_{-D}^{D} d\varepsilon_{\mathbf{k}}\frac{n_F\left(\omega_{\mathbf{k}}(+)\right) - n_F\left(\omega_{\mathbf{k}}(-)\right)}{\sqrt{\left(\varepsilon_{\mathbf{k}} - \widetilde{E}_f\right)^2 + 4V^2 D_\sigma}}, \quad (9)$$

where the values $\omega_{\mathbf{k},\sigma}(\pm)$ are the poles of the GF, given by

$$\omega_{\mathbf{k},\sigma}(\pm) = \frac{1}{2}\left\{\left(\varepsilon_{\mathbf{k},\sigma} + \widetilde{E}_f\right) \pm \sqrt{\left(\varepsilon_{\mathbf{k},\sigma} - \widetilde{E}_f\right)^2 + 4V^2 D_\sigma}\right\}. \quad (10)$$

In the present paper we adopt a schematic classification proposed by Varma [43] and recently reintroduced by Steglich et al. [44,45], which illustrates the competition between magnetic order and Fermi liquid formation. This classification is given in terms of the dimensionless coupling constant for the exchange between the local f spin and the conduction-electron spins, given by $g = \rho_c(\mu)|J_K|$. The J_K is the Kondo coupling constant, connected to the parameters of the PAM via the Schrieffer-Wolff transformation [46] that gives $J_K = 2V^2/|E^o_f - \mu|$ when $U \to \infty$. Within the SBMFT or the X-boson we then have that

$$g = \rho_c(\mu)|J_K| \ \sim \frac{V^2}{D|E^o_f - \mu|}, \quad (11)$$

where for simplicity we take $\rho_c(\mu) = 1/2D$. The qualitative behavior of the exemplary Ce-based compounds is related to this parameter as follows: when $g > 1$, the compound presents an intermediate valence (IV) behavior, while for $g < 1$ it is in a heavy fermion Kondo regime (HF). There exists a critical value g_c at which the Kondo and the RKKY interactions have the same strength, and non Fermi-liquid (NFL) effects have been postulated when $g = g_c$. For $g_c < g < 1$, the magnetic local moments are not apparent at very low temperatures and the system presents a Fermi liquid behavior, while for $g < g_c$ the system is in the local magnetic moment regime (LMM). We point out that the parameter g classifies the regimes of the PAM only in a very qualitative way. Finally, in its present form the X-boson approach includes hybridization effects only to second order in V, and the self-energy does not depend on the wave vector. We then conclude that there is no RKKY interaction within the present approximation, and we cannot discuss the non-Fermi liquid behavior, nor find the value of g_c.

3 Calculation of the properties

3.1 Specific heat

To calculate the specific heat employing Ω we first show by standard thermodynamic techniques that the entropy S is given by

$$S = -\left(\frac{\partial F}{\partial T}\right)_{N_t,V} = -\left(\frac{\partial \Omega}{\partial T}\right)_{\mu,V}. \quad (12)$$

Assuming a conduction band with constant density of states and width $W = 2D$ and in the absence of magnetic field, we find from equations (5, 6) that

$$S = S_o + S_{FL}, \quad (13)$$

with

$$S_o = N_s\left[\ln\left(\frac{1 + 2\beta\exp(\beta\widetilde{\varepsilon}_f)}{(1+\exp(\beta\widetilde{\varepsilon}_f))^2}\right) - \frac{2\beta\widetilde{\varepsilon}_f}{1 + n_F\left(\widetilde{\varepsilon}_f\right)}\right], \quad (14)$$

and

$$S_{FL} = \frac{1}{D}\sum_{\ell=\pm}^{2}\int_{-D}^{D} dx\ \omega_\ell(x)\ n_F\left(\omega_\ell(x)\right) + \ln\left[1+\exp\left(\beta(\omega_\ell(x))\right)\right], \quad (15)$$

and then that

$$C_v = T\left(\frac{\partial S}{\partial T}\right)_{N_t,V} = -T\ \left(\frac{\partial^2 \Omega}{\partial T^2}\right)_{\mu,V} + T\ \left(\frac{\partial \mu}{\partial T}\right)_{N_t,V}\ \left(\frac{\partial N}{\partial T}\right)_{\mu,V}, \quad (16)$$

with

$$-T\ \left(\frac{\partial^2 \Omega}{\partial T^2}\right)_{\mu,V} = -T\ \left(\frac{\partial^2 \overline{\Omega}_0}{\partial T^2}\right)_{\mu,V} + \frac{k_B\,\beta^2}{D}\sum_{\ell=\pm}^{2}\int_{-D}^{D} dx\ \omega_\ell^2(x)\ n_F\left(\omega_\ell(x)\right)\left[1-n_F\left(\omega_\ell(x)\right)\right] - T\ N_s\left(\frac{\partial^2(\Lambda(R-1))}{\partial T^2}\right)_{\mu,V}, \quad (17)$$

where

$$\omega_\pm(x) = \frac{1}{2}\left(x+\widetilde{\varepsilon}_f\right) \pm \frac{1}{2}\sqrt{\left(x-\widetilde{\varepsilon}_f\right)^2 + 4\left|V\right|^2 D_\sigma} \quad (18)$$

and

$$-\ T\ \left(\frac{\partial^2 \overline{\Omega}_0}{\partial T^2}\right)_{\mu,V} = -2N_s\ k_B\ \beta^2\widetilde{\varepsilon}_f^2\ \exp(\beta\widetilde{\varepsilon}_f) \times \frac{\left[3+2\exp(\beta\widetilde{\varepsilon}_f)\right]}{\left[\exp(\beta\widetilde{\varepsilon}_f)+2\right]^2\left[\exp(\beta\widetilde{\varepsilon}_f)+1\right]^2}. \quad (19)$$

3.2 Electrical resistivity

The static conductivity $\sigma_{dc}(T)$ is obtained considering the limit of the dynamical conductivity $\omega \to 0^+$ for $\sigma(\omega, T)$ [27] and is given by

$$\sigma_{dc}\left(T\right) = \frac{1}{2D}\int_{-\infty}^{\infty} d\omega\left(-\frac{dn_F(\omega)}{d\omega}\right)\int_{-D}^{D} d\varepsilon\ \left(\rho_{c,\sigma}(\omega;\varepsilon)\right)^2, \quad (20)$$

where $\beta = 1/k_B T$ with k_B being the Boltzmann constant, n_F is the Fermi distribution and the conduction density of states is given by

$$\rho_{c,\sigma}(\omega;\varepsilon) = \frac{1}{\pi}\ \lim_{\eta\to 0}\ Im\left\{G_{cc,\sigma}(\mathbf{k},\omega+i\left|\Gamma\right|)\right\}, \quad (21)$$

where the conduction Green function $G_{cc,\sigma}$ is given by equation (3). The static resistivity is obtained inverting equation (20)

$$\rho_{dc}(T) = \frac{1}{\sigma_{dc}\left(T\right)}. \quad (22)$$

Notice that this expression for the conductivity must be used with care. In the problem considered here, there is translational invariance and consequently $\boldsymbol{k}$ is a good quantum number. However in real systems, impurity scattering is always present and this limits the electron mean free path. In the numerical calculations, this is taken into account by including a finite lifetime for the conduction electrons. Formally this is done by replacing, $\omega \to \omega + i\Gamma$, in the conduction Green's functions [47], where Γ is considered temperature independent. We pointed out that here we are interested in the temperature dependence of the conductivity which is not affected by the magnitude of Γ. We would like to stress, that this procedure is necessary because the X-boson approach does not present finite lifetime effects in its Green's functions, in consequence the method is not adequate to describe the intermediate to high temperature effects of the FeSi. For this reason we restrict our analysis to the low temperature regime of the PAM. The numerical calculation of the conductivity, at low temperatures, must be taken with care because the integral in equation (20) is performed over the very peaked functions and it is necessary to find the position of each peak in each stage of the integration to obtain a reliable result.

3.3 Magnetic susceptibility

To calculate the magnetic susceptibility χ we apply an external magnetic field $\boldsymbol{h}$ along the z direction and we employ the general thermodynamic relation

$$\chi = \left(\frac{\partial \boldsymbol{M}}{\partial \boldsymbol{h}}\right)_{N_t,V} = -\frac{1}{V}\left(\frac{\partial^2 F}{\partial h^2}\right)_{N_t,V}, \quad (23)$$

where F is the Helmholtz free energy

$$F = \Omega + \mu N_t, \quad (24)$$

and the expression for the grand thermodynamic potential Ω is given by equation (5), but with the energies modified by the external magnetic field

$$\omega_{\mathbf{k},\sigma}(\pm) = \omega_{\mathbf{k},\sigma}(\pm) - \boldsymbol{\sigma}.\boldsymbol{h}. \quad (25)$$

The susceptibility is obtained through equations (5) and (23, 24)

$$\chi = \chi_o + \chi_{FL}, \quad (26)$$

with the zero order and Fermi-liquid magnetic susceptibilities given by

$$\chi_o = -\frac{\beta}{2}\frac{n_F^2}{(1+n_F)}, \quad (27)$$

$$\chi_{FL} = \frac{-\beta}{4}\sum_{\boldsymbol{k},l=\pm}\ sech^2\left[\frac{1}{2}\left(\beta\omega_{\boldsymbol{k}\sigma}(l=\pm)\right)\right], \quad (28)$$

where n_F is the Fermi distribution function and the quasiparticle energies $\omega_{\boldsymbol{k}\sigma}(l=\pm)$ are given by equation (25).

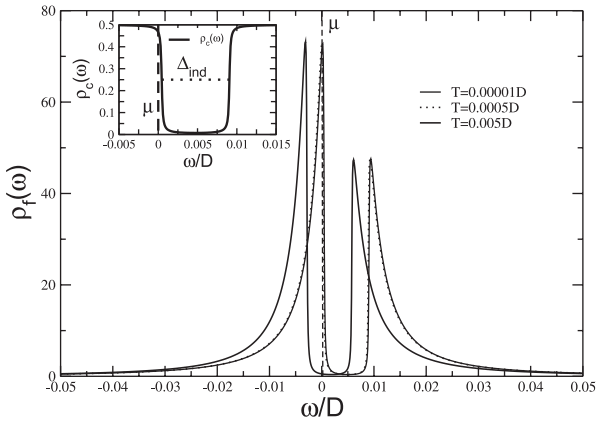

Fig. 1. Density of states for the localized f electrons $\rho(\omega)$ as function of the energy ω, using the following set of parameters $E_f = -0.15D$, $V = 0.08D$ and total number of particles per site $N_t = 1.55$.

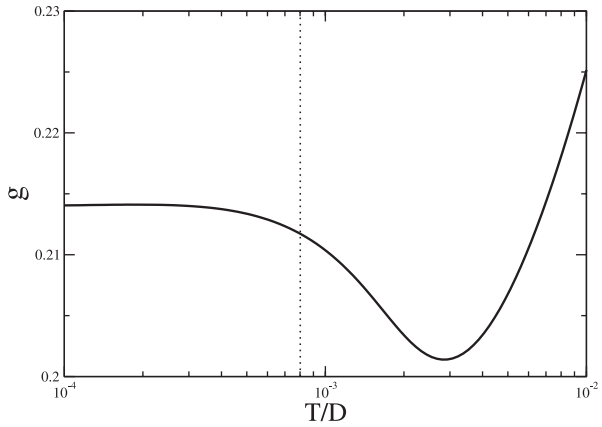

Fig. 2. Evolution of the Steglich's parameter g vs. T, at low temperatures, when the chemical potential μ is located inside the gap and enters the metallic region. The dashed line indicates the temperature where the insulator-metal transition occurs.

4 Results and discussion

We consider the impurity band an important ingredient to elucidate the properties of the compound FeSi, because the localized states in the gap can drive the chemical potential toward the conduction band, but we concentrate the discussion of the paper in the strong correlation mechanism that also drives the movement of the chemical potential to cross the conduction band. In the real compound these two mechanism probably act together but from the theoretical point of view it is not easy to consider, at the same time, the roles of the disorder and the correlation. Thus we concentrate the paper on the study of the correlation effects. As FeSi is a highly correlated semiconductor, we have employed the Anderson model to parametrize the compound. We work with the Anderson model, in the limit of $U \to \infty$, which was suggested by Aeppli and Fisk [1] as an especially interesting limit to describe the Kondo insulator FeSi. In this model, the total number of electrons per site Nt, varies from $Nt = 0$ to 3 electrons, one localized and highly correlated and the other two uncorrelated (conduction electrons). As it happens with the Anderson model, the hybridization opens a gap in the density of states and in the intermediate valence regime, this gap occurs approximately in the region where $Nt = 1.5$–1.6 (FeSi is an intermediate valence compound [13]). For this reason we chose in all the calculations, $Nt = 1.55$ to have the chemical potential localized inside the gap. But by varying the temperature, the correlation effects, drive the chemical potential through the gap and, at low temperatures, the chemical potential crosses the gap and enters the conduction band. The same effect can be obtained alloying the system. This movement of the chemical potential is not present in the intrinsic semiconductors, in which the chemical potential is pinned inside the gap.

In Figure 1 we present the density of states of the localized f electrons as function of the energy using the following parameters set $E_f = -0.15D, V = 0.08D$. In each step of the numerical calculations the total number of particles per site remains constant, and the chemical potential μ is varied at each T until obtaining a fixed $N_t = 1.55$. At intermediate temperatures the chemical potential ($\mu = 0.0$ in Fig. 1) is located inside the gap (see curve corresponding to $T = 0.005D$), but as the temperature decreases, the chemical potential crosses the gap and at the temperature $T \simeq 0.0008D$ enters the conduction band. At this temperature the system suffers an insulator-metal transition due to the strong correlations; the localized and conduction occupation numbers are practically constant and assume the values $n_f = 0.665$ and $n_c = 0.885$ respectively. This value of n_f corresponds to an intermediate valence situation. The variation of the occupation numbers are only relevant for $T > T_{KL}$, but as the X-boson does not incorporate finite lifetime effects we exclude this region from our analysis.

In Figure 1, at very low temperatures, μ enters a region of a huge density of states as we can see from the curves corresponding to $T = 0.0005D$ and $T = 0.00001$. In the inset of the figure we plot the density of states of conduction c electrons as function of the energy, as in the ρ_f curve the chemical potential is located at zero and we indicate the magnitude of the indirect gap $\Delta_{ind} = 0.008541D$, which is given approximately by the equation $\Delta_{Ind} = \frac{\pi V^2 D_\sigma}{2D} \sim 9.0 \times 10^{-3} D$ and is associated with the transport properties of the system.

In Figure 2 we present the evolution of the Steglich's parameter g, as we decrease the temperature, calculated with equation (11), and in this very low temperature regime $g = 0.214$, the ground state of the system is metallic and exhibits a heavy fermion character. The dashed line indicates the temperature where the insulator-metal transition occurs.

In Figure 3 we present the derivative of $(dn_{fc}/dT) = \left(d\langle c^\dagger_{i\sigma} f_{i\sigma}\rangle/dT\right)$ vs. T, for the same set of parameters given in Figure 1. We define the lattice Kondo temperature according to our previous paper [36]. Bernhard et al. [48], defined a lattice Kondo temperature T_K (we call it T_{KL} in this work) as equal to the T corresponding to the minimum of the temperature derivative of the average $\langle c^\dagger_{i\sigma} f_{i\sigma}\rangle$,

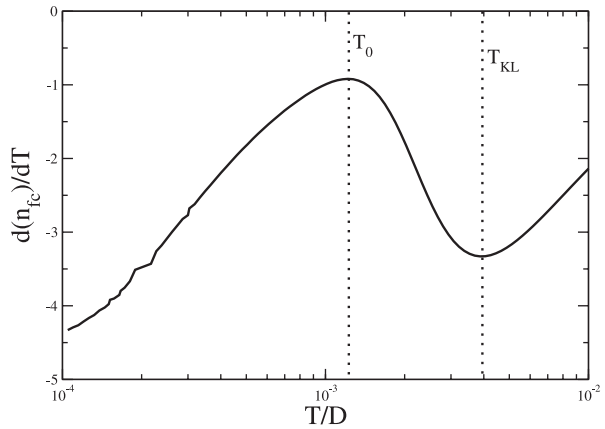

Fig. 3. Derivative of (dn_{fc}/dT) vs. T, for the same set of parameters given in Figure 1. We indicate by the dotted lines the coherence and Kondo temperatures, respectively $T_0 = 0.0012D$ and $T_{KL} = 0.0039D$.

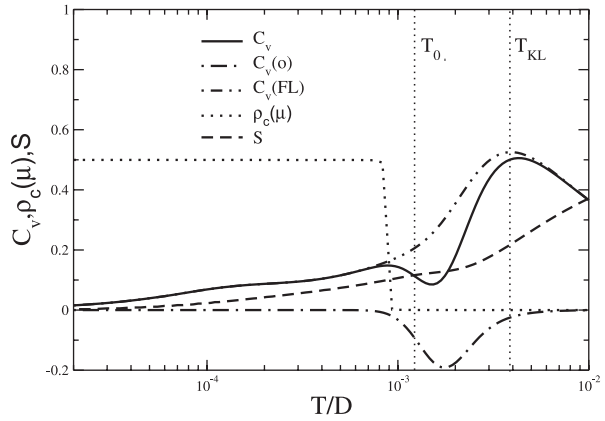

Fig. 4. Specific heat C_v, entropy S and conduction density of states at the chemical potential $\rho_c(\mu)$ vs. T using the same parameters set of Figure 1.

that measures the "transference" of electrons from the localized levels to the conduction band and vice-versa. On the other hand, Peres et al. [49], define a correlation temperature T^* (we call it T_0 and we identify this temperature as the coherence temperature), equal to the T corresponding to the maximum of the temperature derivative of the parameter $\langle c^\dagger_{i\sigma} f_{i\sigma}\rangle$. From the figure we obtain the following values for the coherence and Kondo temperatures respectively $T_0 = 0.0012D$ and $T_{KL} = 0.0039D$.

In Figure 4 we present the different contributions of the specific heat C_v, the entropy S and the conduction density of states at the chemical potential $\rho_c(\mu)$ vs. temperature T using the same parameters set of Figure 1. Although it is C_p that is generally measured, the difference $C_p - C_v$ is usually small in liquids and solids, and shows a dependence with T similar to that obtained with the C_p of FeSi, (see for example the experimental works of Jacarino and co-workers [6] and Paschen et al. [10]), that measured C_p in the very low temperature region. From this figure we can approximately identify the low temperature regimes that emerge from the experimental results [7–12]. In the range $T_{KL} > T > T_0$, we identify the regime characterized by an activation energy and for $T < T_0$, we have a regime characterized by the formation of coherent states. The zero order contribution to $C_v(0)$ is always negative and mainly contributes to the activated regime, whereas the Fermi-liquid contribution $C_v(FL)$ dominates all the temperature range. At temperatures below $T = 0.0008D$, the chemical potential crosses the gap and enters the conduction band generating a reentrant metallic ground state.

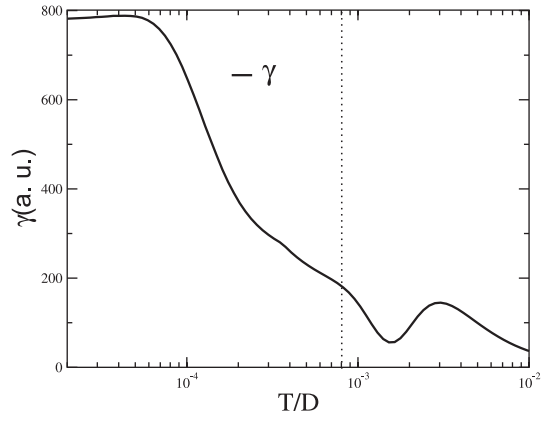

Fig. 5. Specific heat coefficient γ vs. T using the same parameters set of Figure 1. The dashed line indicates the temperature where the insulator-metal transition occurs.

We showed in a previous paper [36], that the entropy per site at low T tends to zero in the heavy Fermion Kondo (HF-K) regime (μ is located in the first peak), corresponding to a singlet ground state, and it tends to $k_B \ln 2$ in the Heavy Fermion Local Magnetic Moment (HF-LMM) regime (μ is located in the second peak), corresponding to a doublet ground state at each site. From the same figure we can see that the entropy S per site tends to zero at low temperatures, and we conclude that the system goes to the Kondo singlet ground-state, while the huge value of density of states f at the chemical potential μ (see Fig. 1) signals the simultaneous appearance of the Kondo resonance.

In Figure 5 we present the γ coefficient of specific heat and we can see a huge increase of this quantity as the chemical potential enters the conduction band. The dashed line indicates where the insulator-metal transition occurs. This result agrees well with the Paschen et al. experimental measurements of this parameter for FeSi [10]. They found an effective-mass ratio of approximately 900, but contrary to their suggestion that the origin of this metallic ground state could be an impurity band formed in the gap with a "spectacularly" narrow band width, we attribute this huge increase of the γ coefficient to the reentrant behavior of μ at low temperatures. The specific heat presents the general structure analyzed in a previous paper [36], but at very low temperatures, when the chemical potential is located inside the conduction band, C_v goes linearly to zero as we can see from Figure 6, where we adjust the theoretical results with the function $C_v = AT$, and we obtain the parameter $A = 785.304$.

In Figure 7 we present the resistivity $\rho_{dc}(T)$ vs. T, with the same parameters of Figure 1. Following Mutou

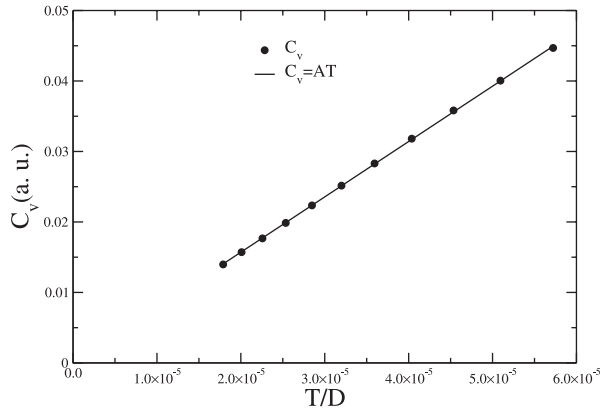

Fig. 6. Adjustment of the low temperature specific heat C_v vs. T, at very low temperatures, when the chemical potential μ is located inside the conduction band. The parameters are the same as Figure 1. We adjust the theoretical points to the formula $C_v = AT$ and we obtain $A = 785.304$.

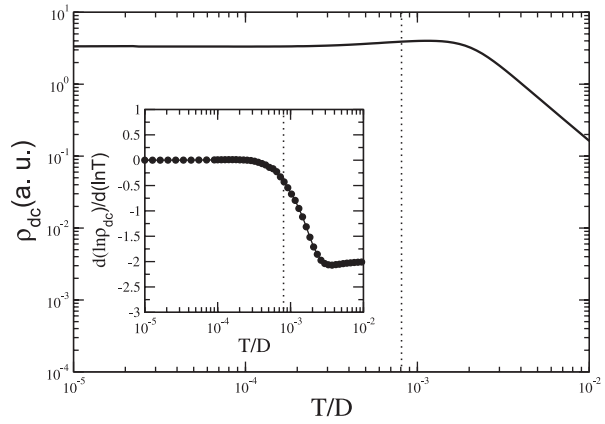

Fig. 7. Resistivity $\rho_{dc}(T)$ vs. T, with the same parameters of Figure 1. In the inset of the figure we present $d(\ln\rho)/d(\ln T) = (d\rho/\rho)/(dT/T)$ vs. T. The dashed line indicates the temperature where the insulator-metal transition occurs.

and Hirashima [47] who introduced a small imaginary part Γ in the GFs $G^{ff}_{\mathbf{k}\sigma}(z)$ and $G^{cc}_{\mathbf{k}\sigma}(z)$, i.e. replacing $z = i\omega$ by $z + i\ \Gamma\ sgn(\omega)$. Their justification is the existence in real systems of scattering processes due to phonons and impurities. In our case we employ the $\Gamma = 0.001$. Our result for the resistivity agrees qualitatively well with several experimental measurements [7–12]. The magnitude of ρ_{dc} saturates at very low temperatures, which is a consequence of the reentrant transition into a metallic state. This conclusion is supported by the resistivity experimental results of Lunkenheimer et al. [9]. They performed measurements of ac conductivity of polycrystalline FeSi at temperatures 80 mK $\leq T \leq$ 450 K and frequencies 20Hz $\leq \nu \leq$ 1 GHz and concluded that at the metallic side, the dominant charge carriers behave as band-like states and there is no signal of hopping conductivity in this regime, and that below 4.5 K the dielectric constant increases by a factor of 10 when the temperature is lowered down to 1.6 K. They concluded that this strong increase could indicate a transition into a metallic state at low temperatures. This

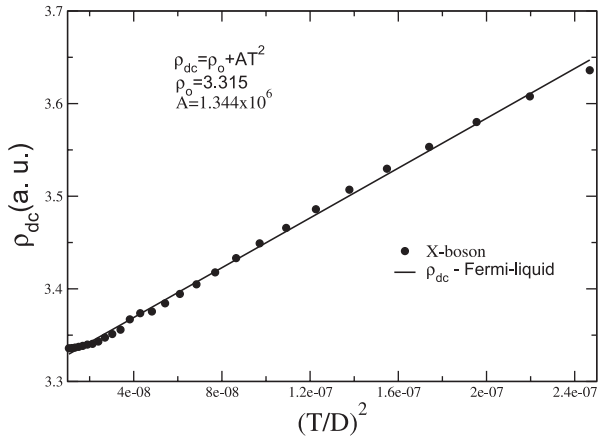

Fig. 8. Adjustment of the low temperature resistivity $\rho_{dc}(T)$ vs. T^2, when the chemical potential μ is located inside the conduction band. The parameters are the same as Figure 1. We adjust the theoretical points to the formula $\rho_{dc}(T) = \rho_0 + AT^2$, with $\rho_0 = 3.315$ and $A = 1.344 \times 10^6$.

interpretation was also suggested by the results of Hunt et al. [8] and Chernikov et al. [11].

The saturation trend of the resistivity ρ_{dc}, at low temperatures, can be described qualitatively by evaluating the behavior of the derivative $d(\ln\rho)/d(\ln T) = (d\rho/\rho)/(dT/T)$ [11,50]. At low temperatures, the conductivity approaches to nonzero values and $d(\ln\rho)/d(\ln T) \rightarrow 0$ as $T \rightarrow 0$. In the inset of Figure 7 we present $d(\ln\rho)/d(\ln T)$ vs. temperature. This result is similar to the experimental results [10,11], the temperature derivative of ρ_{dc} is negative over the whole temperature range and tends to zero at low temperatures, but contrary to the Paschen et al. results [10], where the curve presents two minimums, in our case the curve presents only one minimum, probably because we do not take into account the impurity band that plays an important role in the intermediate temperature range.

In Figure 8 we present the adjustment of the low temperature resistivity $\rho_{dc}(T)$ vs. T^2, at very low temperatures, when the chemical potential μ is located inside the conduction band. The parameters are the same as Figure 1. We adjust the theoretical points to the formula $\rho_{dc}(T) = \rho_0 + AT^2$, with $\rho_0 = 3.315$ and $A = 1.344 \times 10^6$. This result indicates that the X-boson approach correctly describes the Fermi-liquid behavior of the resistivity at very low temperatures.

In Figure 9 we present the electrical conductivity as function of temperature. In the inset of the same figure we present the adjustment of the conductivity in the activated region to the formula $\sigma_{dc} = \sigma_o \exp(-\Delta_\sigma/T)$, with $\sigma_o = 8.11$ and $\Delta_\sigma = 0.0082D$, which agrees very well with the indirect gap of the density of states $\Delta_{ind} = 0.0085D$, as indicated in the inset of Figure 1.

In Figure 10 we present the different contributions to the static susceptibility and the f localized density of states at the chemical potential $\rho_f(\mu)$. The magnetic susceptibility follows the same low temperature regimes indicated by the experimental results [7–12] and the zero order contribution χ_o is only relevant in the temperature

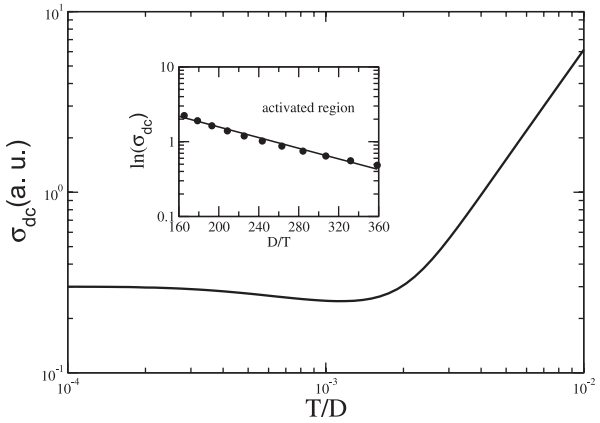

Fig. 9. Conductivity $\sigma_{dc}(T)$ vs. T, with the same parameters of Figure 1. In the inset of the figure we present the conductivity $\sigma_{dc}(T)$ in the activated region vs. T.

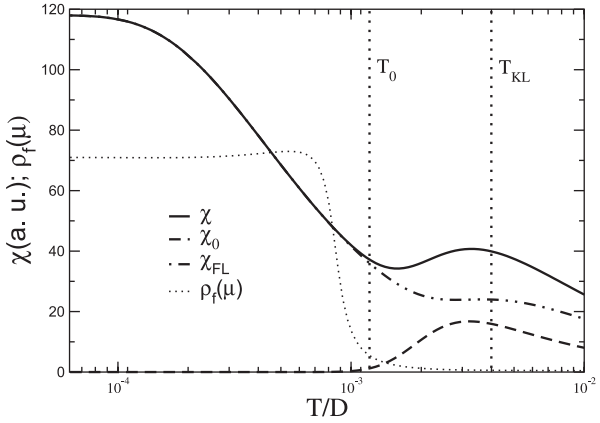

Fig. 10. Susceptibility χ and localized density of states at the chemical potential $\rho_f(\mu)$ vs. T using the same parameters of Figure 1.

interval $T > T_0$, whereas the Fermi-liquid contribution χ_{FL} dominates the susceptibility in all the regimes. After the chemical potential μ enters the conduction band, the susceptibility presents a huge increase (see $\rho_f(\mu)$ in the same figure), and as in the case of C_v analyzed in Figure 4, this region is characterized by the coherent regime $T < T_0$, and at very low temperatures it attains a saturation limit characteristic of the Pauli-like contribution. This behavior indicates a full compensation of the magnetic moments by the conduction electrons, characteristic of the Kondo behavior of the system in this temperature range. But the experimental results [8,10] in this region, indicate a divergent behavior of the $\chi(T)$ as $T \to 0$, which can be an indication that the ground state of the FeSi, is not so simple, with part of the magnetic moments interacting between themselves and part remaining paramagnetic down to at least 50 mK [10].

In Figure 11 we present the susceptibility χ and insets of the different low temperature susceptibilities regimes of the model vs. temperature T. In the inset (a) we present the fitting of the Curie-Weiss law $\chi = C/(T - \Theta)$ for the very low temperature regime ($T < T_o$), and we obtain the following parameters set for this region: $C = 0.05310D$

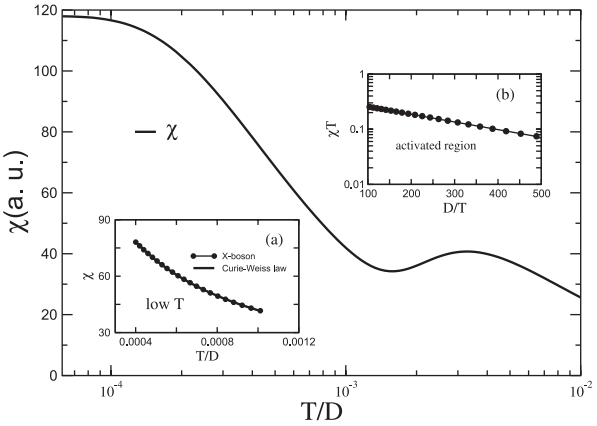

Fig. 11. Susceptibility χ vs. T and insets of the low temperature susceptibility regimes of the model, using the same parameters of Figure 1.

and $\Theta = -0.0002890D$, with $\Theta < 0$, which is an indication of the presence of anti-ferromagnetic correlations which agrees well with experimental observations of the increase of susceptibility following the Curie-Weiss law, in this temperature range [8,10]. In the inset (b) of Figure 5 we consider the thermal activated region ($T_o < T < T_{KL}$) and we fit the theoretical results with the same function employed to fit the experimental results [8,10], $\chi = \frac{C_o}{T} \exp(-\frac{\Delta_\chi}{T})$, where Δ_χ is the magnetic gap. We obtain the following parameters set for this region: $C_o = 0.3543D$ and $\Delta_\chi = 0.0032D$, with $\Theta < 0$.

5 Summary and conclusions

In this paper we study the low temperature properties of Kondo insulators employing the X-boson method [34,35] to study the PAM in the limit of infinite Coulomb repulsion $U \to \infty$. In particular we choose a set of parameters adequate to describe the FeSi and we study the system in the low temperature regime where the hybridization gap is completely open. The model is consistent with the experimental results of several works [7–12]. We propose a scenario where the low temperature properties are governed by a reentrant transition into a metallic state, at very low temperatures. In our case the insulator-metal transition in FeSi is driven by strong Coulomb correlations that occur when the chemical potential crosses the gap and enters the conduction band generating a metallic ground state.

As we have discussed earlier, we do not consider the role of the impurity band in the gap of FeSi, although we consider that it is an important ingredient to explain the behavior of the system in the low temperature region. The finite localized density of states generated inside the gap by the impurity band contributes to the specific heat and the susceptibility and due to the existence of localized states, the impurity band can change the position of the chemical potential and the behavior of the electrical conductivity.

The metallic ground state presents the general characteristics of Fermi-liquids: linear specific heat, resistivity

following a T^2 law and Pauli-like susceptibility as we can see from Figures 6, 8 and 10, but with heavy quasiparticles as we can infer from the huge γ coefficient presented in Figure 5 and from the saturation value of the static susceptibility at very low temperatures, which indicates a full compensation of the magnetic moments by the conduction electrons, characteristic of the Kondo behavior of the system in this temperature range. We can stress that the present treatment only furnishes a qualitative description of the low temperature regime of the Kondo insulator FeSi. As discussed in the text, the X-boson does not incorporate finite lifetime effects and we do not take into account the role of the impurity band inside the gap, but we recover the general behavior of several properties of the very low temperature regime of the compound [7–12].

We acknowledge the financial support of the Colombia National University, projects DINAIN:20601003550 and DIB:8003060, Colombian agency COLCIENCIAS-project: 1101-333-18707, CNPq (Brazilian National Research Council) and FAPERJ (Rio de Janeiro State Research Foundation) from the grant "Primeiros Projetos"

References

1. G. Aeppli, Z. Fisk, Comments Condens. Matter Phys. **16**, 155 (1992)
2. L. Degiorgi, Rev. Mod. Phys. **71**, 687 (1999)
3. P. Wachter, in *Handbook on the Physics and Chemistry of Rare Earths*, edited by K.A. Gschneidner Jr, L. Eyring, G.H. Lander, G.R. Choppin (Elsevier, Amsterdam 1994), Vol. **19**
4. P.S. Riseborough, Adv. Phys. **49**, 257 (2000)
5. C.H. Park, Z.X. Shen, A.G. Loeser, D.S. Dessau, D.G. Mandrus, A. Migliori, J. Sarrao, Z. Fisk, Phys. Rev. B. **52**, 16981(R) (1995)
6. V. Jaccarino, G.K. Wertheim, J.H. Wernick, L.R. Walker, Sigurds Arajs, Phys. Rev. B **160**, 476 (1967)
7. Z. Schlesinger, Z. Fisk, Hai-Tao Zhang, M.B. Maple, J.F. DiTusa, G. Aeppli, Phys. Rev. Lett. **71**, 1748 (1993)
8. M.B. Hunt, M.A. Chernikov, E. Felder, H.R. Ott, Z. Fisk, P. Canfield, Phys. Rev. B. **50**, 14933 (1994)
9. P. Lunkenheimer, G. Knebel, R. Viana, A. Loidl, Solid State Communications **93**, 891 (1995)
10. S. Paschen, E. Felder, M.A. Chernikov, L. Degiorgi, H. Schwer, H.R. Ott, D.P. Young, J.L. Sarrao, Z. Fisk, Phys. Rev. B **56**, 12916 (1997)
11. M.A. Chernikov, L. Degiorgi, E. Felder, S. Paschen, A.D. Bianchi, H.R. Ott, J.L. Sarrao, Z. Fisk, D. Mandrus, Phys. Rev. B **56**, 1366 (1997)
12. N. Sluchanko, V. Glushkov, S. Demishev, L. Weckhuysen, V. Moshchalkov, A. Menovsky, JETP Lett. **68**, 817 (1998)
13. C.M. Varma, Phys. Rev. B **50**, 9952 (1994)
14. Ncholu Manyala, Yvan Sidis, J.F. Ditusa, Gabriel Aeppli, D.P. Young, Zachary Fisk, Nature Materials **3**, 255 (2004)
15. N. Manyala, Y. Sidis, J.F. Ditusa, G. Aeppli, D.P. Young, Z. Fisk, Nature **404**, 581 (2000)
16. V.V. Glushkov, I.B. Vorkoboinikov, S. Demishev, I.V. Krivitiskii, A. Menovsky, V. Moshchalkov, N.A. Samarin, N.E. Sluchanko, J. Exp. Theor. Phys. **90**, 394 (2004)
17. N. Sluchanko, V. Glushkov, S. Demishev, L. Weckhuysen, V. Moshchalkov, A. Menovsky, J. Mag. Mag. Mat. **258–259**, 222 (2003)
18. L. Degiorgi, M.B. Hunt, H.R. Ott, M. Serssel, B.J. Feentra, G. Grüner, Z. Fisk, P. Canfield, Europhys. Lett. **28**, 341 (1994)
19. P. Schlottmann, Phys. Rev. B **46**, 998 (1992)
20. Solid State Commun. **74**, 735 (1990)
21. E. Arushanov, M. Respaud, J.M. Broto, J. Leotin, S. Askenazy, Ch. Kloc, E. Bucher, K. Lisunov, Phys. Rev. B **55**, 8056 (1997)
22. H. Kamimura, Philos. Mag. B **42**, 763 (1980)
23. L. Peche, E.V. Anda, C.A. Büsser, Phys. Rev. B **68**, 245119 (2003)
24. M.F. Hundley, P.C. Canfield, J.D. Thompson, Z. Fisk, Phys. Rev. B **50**, 18142 (1994)
25. A. Latge, E.V. Anda, Solid State Communications **76**, 1387 (1990)
26. M.J. Rozenberg, G. Kotliar, H. Kajueter, Phys. Rev. B **54**, 8452 (1996)
27. M.E. Foglio, M.S. Figueira, Phys. Rev. B **60**, 11361 (1999)
28. M.E. Foglio, M.S. Figueira, Phys. Rev. B **62**, 7882 (2000)
29. P. Coleman, Phys. Rev. B. **29**, 3035 (1984); M. Newns, N. Read, Advances in Physics **36**, 799 (1987)
30. C. Sanchez-Castro, K.S. Bedell, B.R. Cooper, Phys. Rev. B **47**, 6879 (1993)
31. P.S. Riseborough, Phys. Rev. B **45**, 13984 (1992)
32. P. Coleman, Phys. Rev. B **35**, 5072 (1987)
33. Tatiana G. Rappoport, M.S. Figueira, M.A. Continentino, Phys. Lett. A **264**, 497 (2000)
34. R. Franco, M.S. Figueira, M.E. Foglio, Phys. Rev. B **66**, 045112 (2002)
35. R. Franco, M.S. Figueira, M.E. Foglio, Physica A **308**, 245 (2002)
36. R. Franco, M.S. Figueira, M.E. Foglio, Phys. Rev. B **68**, 205108 (2003)
37. T. Lobo, M.S. Figueira, R. Franco, J. Silva-Valencia, M.E. Foglio, Physica B: Condensed Matter, to be published (2007)
38. C. Fu, S. Doniach, Phys. Rev. B **51**, 17439 (1995)
39. M.S. Figueira, M.E. Foglio, G.G. Martinez, Phys. Rev. B **50**, 17933 (1994)
40. M.E. Foglio, M.S. Figueira, J. Phys. A. Math. Gen. **30**, 7879 (1997)
41. J. Hubbard, Proc. R. Soc. London, Ser. A **276**, 238 (1964)
42. S.G. Ovchinnikov, V.V. Valkov, Hubbard Operators in *The Theory Of Strongly Correlated Electrons* (Imperial College Press, 2004)
43. C.M. Varma, Comments on Condensed Matter Physics **11**, 221 (1985)
44. N. Grewe, F. Steglich, *Handbook on the Physics, Chemistry of Rare Earths*, edited by K.A. Gschneider Jr, L. Eyring (Elsevier, Amsterdam, 1991), p. **14**
45. F. Steglich, C. Geibel, K. Gloss, G. Olesch, C. Schank, C. Wassilew, A. Loidl, A. Krimmel, G.R. Stewart, J. Low Temp. Phys. **95**, 3 (1994)
46. J.R. Schrieffer, P.A. Wolff, Phys. Rev. **149**, 491 (1996)
47. T. Mutou, D.S. Hirashima, J. Phys. Soc. Jpn **63**, 4475 (1994)
48. B.H. Bernhard, C. Lacroix, J.R. Iglesias, B. Coqblin, Physica B **259–261**, 227 (1999); B.H. Bernhard, C. Lacroix, Phys. Rev. B **60**, 12149 (1999)
49. N.M.R. Peres, P.D. Sacramento, M.A.N. Araujo, Phys. Rev. B. **64**, 113104 (2001)
50. A. Mobius, Solid State Communications, **73**, 215 (1990)